IEEE Access
Multidisciplinary | Rapid Review | Open Access Journal

Received April 23, 2019, accepted May 13, 2019, date of publication May 16, 2019, date of current version June 4, 2019.

Digital Object Identifier 10.1109/ACCESS.2019.2917316

Trim Strategy, Control Model, and Flight Dynamics Characteristics of Canard Rotor/Wing Aircraft in Transition Mode

HONGGANG GAO, ZHENGHONG GAO, YANG NA, AND CHAO PANG
School of Aeronautics, Northwestern Polytechnical University, Xi'an 710072, China
Corresponding author: Zhenghong Gao (zgao@nwpu.edu.cn)

ABSTRACT The transition mode of canard rotor/wing (CRW) aircraft is complex and important. During the transition flight, components that generate lift are transferred from one to another, in addition, the redundancy of control system may induce control conflict even plane crash if they don't cooperate well. It is significant to investigate the trim strategy, redundant control, and flight dynamics characteristics of CRW during transition flight. First, aerodynamic forces and moments were calculated by combining the blade element theory, computational fluid dynamics (CFD) and engineering estimation, and the motion equations of CRW in transition mode are established. Next, by analyzing the principle of transition flight, a trim strategy is proposed, and the trim results are credible and reasonable. Then, a control model for solving redundant control is proposed, which can realize simple and effective control during the transition process. Finally, by analyzing the eigenvalues, it is found that the stability of most modes grows with the increase of forwarding flying speed in the transition process, whereas the variation of minority modes is complicated. The results demonstrate the complexity of dynamic characteristics of CRW in transition mode. The trim strategy and control model and the analysis of the dynamic characteristics in the paper can be used for the subsequent control system design and overall optimization design.

INDEX TERMS Canard rotor/wing aircraft, transition scheme, model building, flight dynamics, control allocation, dynamics analysis.

I. INTRODUCTION

Canard rotor/wing (CRW) aircraft combines the hover and low-speed flight characteristics of helicopters with the high-speed cruising characteristics of fixed-wing aircrafts [1], [2], which is promising in both military and civil fields. Simultaneously, a complicated mode of transition in achieving this combination is involved.

CRW has three flight modes: helicopter mode with the ability to take off and land vertically, fixed-wing mode with high-speed capability, and the transition mode between these two modes [1], [3]. From the perspective of the source of lift, transition mode is a transformation process between the main rotor thrust and the lift generated by the fixed wings. There is also a transfer of control authority between helicopter control system and fixed-wing control system during the transition process.

Various studies on the CRW aircraft have been implemented. Bass *et al.* [4] studied the aerodynamic characteristics of CRW aircraft in helicopter mode and fixed-wing mode via wind tunnel tests. He *et al.* [5] and Deng *et al.* [6] studied the aerodynamic interference between the main rotor and fixed wings based on wind tunnel tests. Sun *et al.* [7], [8] explored the aerodynamic characteristics of the aerofoil of main rotor using computational fluid dynamics (CFD). Pandya and Aftosmis [9] investigated the aerodynamic load change of CRW via non-viscous numerical simulation during transition from helicopter to fixed-wing mode. Kong *et al.* [10] examined the performance characteristics of CRW's propulsion system during flight mode conversion. But only a few researches were conducted on the CRW transition [9], [10], and there is no research on CRW trimming and redundant control during transition process.

How to realize the smooth transfer of the lift surface and the authority of the control system during the CRW transition is a hard work. In addition, the stability analysis of CRW during the transition process is of great significance to the control system design. So, the trimming method, control model and stability analysis of CRW in the transition process are studied in this paper.

The associate editor coordinating the review of this manuscript and approving it for publication was Chaoyong Li.

FIGURE 1. CRW aircraft studied in the paper.

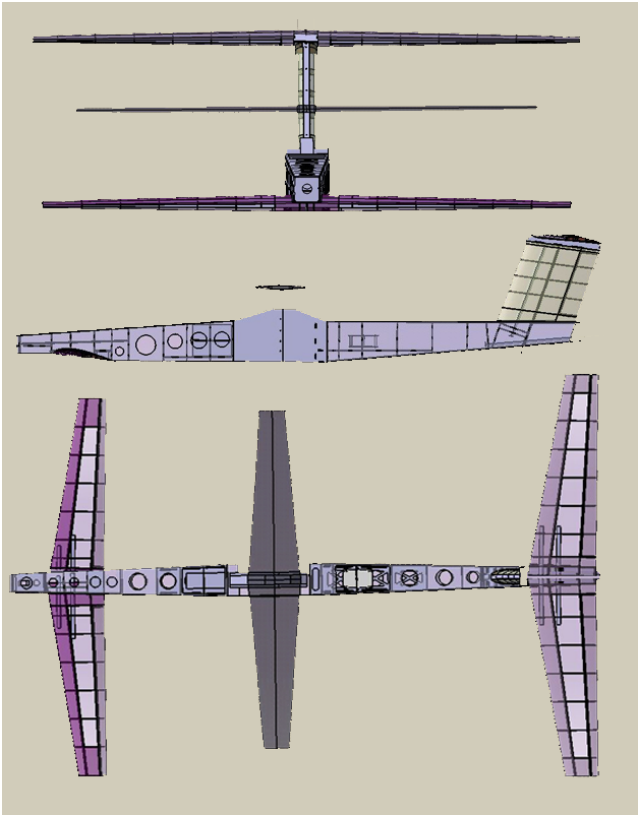

FIGURE 2. Three-view diagram of CRW aircraft in the paper.

The CRW aircraft investigated in the study is shown in Fig. 1 and Fig. 2. Its three flight modes are as follows: (1) The helicopter mode is similar to a conventional helicopter, which has a single main rotor with a tail rotor. It is driven by a motor. (2) The fixed-wing mode is a three-surface aircraft with the main rotor locked as a fixed wing surface, and the propeller at the nose of the CRW provides thrust. (3) The transition mode, which is a process of switching between helicopter mode and fixed-wing mode. In this study, the transition scheme of CRW is first proposed based on the previous flight test experiences and the characteristics of the CRW aircraft. The aerodynamic forces and moments of the main rotor and tail rotor system were calculated by blade element theory [11], [12]. The aerodynamic interactions among components are hard to acquire by mechanism analysis. CFD [7], [8] is employed to obtain the aerodynamic forces and moments of the canard wing, horizontal tail, vertical tail and fuselage under the downwash of the main rotor. The flight dynamics model of the CRW aircraft in transition mode is established based on the above results. Next, a trim strategy is proposed by analyzing the principle of transition flight. Then, a control model is developed to solve the redundant of control system. Finally, the variation of stability during transition is analyzed.

II. FLIGHT DYNAMICS MODELLING OF THE CRW AIRCRAFT IN TRANSITION MODE

The aerodynamic force and moment of aircraft vary with flight state. CRW can have many transition schemes, and the flight state of each way is different. Therefore, the transition scheme is must proposed first to determine the flight state of CRW during transition before developing the flight dynamics model.

A. TRANSITION SCHEME OF THE CRW AIRCRAFT

At present, in the research of CRW transition scheme, Gai *et al.* [13] realized the transition via accelerating forward flight in helicopter mode with a negative pitch angle until a certain speed is reached. Then, it nosed up and started converting. Finally, the main rotor stopped and locked as a fixed wing surface. This way of transition brings a challenge on the structural strength of the fuselage, as in the accelerating process, excessive negative angle of attack (AOA) leads to downward aerodynamic forces generated by the canard wing and horizontal tail, while the thrust of main rotor is upward.

The CRW in Fig.1 has two sets of power systems. In helicopter mode, the power is provided by the main rotor, and in fixed-wing mode thrust is provided by the propeller at the nose of the CRW. The transition scheme in Fig.3 is designed based on the features of the CRW and the previous flight tests experiences. According to a principle of simple and smooth, the transition process of CRW is designed to maintain straight flight at a constant altitude with zero AOA. The canard wing and horizontal tail are designed with constant positive installation angles. The main rotor just provides vertical lift in the transition process. With increasing forward flight speed, the lift generated by the canard wing and horizontal tail grows, and the collective pitch decreases correspondingly, thus can ensure that the resultant lift of the main rotor, canard wing and horizontal tail equal to the aircraft's gravity. The collective pitch of main rotor decreases to zero at the end of the transition process. As the CRW adopts symmetric aerofoils [7], [14], the main rotor produces no lift now, and the lift is completely provided by the canard wing and horizontal tail. The power of the main rotor can be cut off now and the main rotor will gradually speed down. It is finally locked at

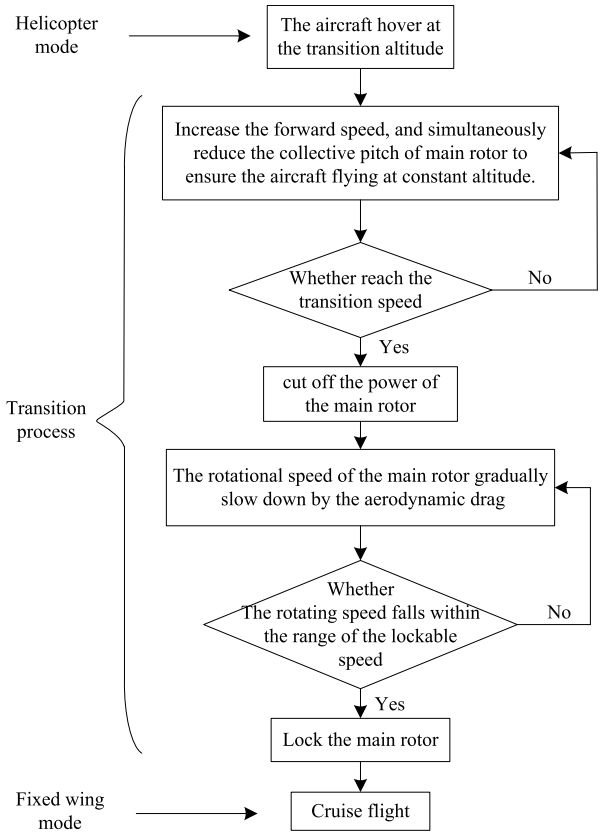

FIGURE 3. Transition process of the CRW aircraft.

TABLE 1. Main parameters of the crw aircraft.

Parameter	Value
Rotor/wing diameter (m)	1.44
Canard span (m)	1.4
Horizon tail span (m)	1.4
Fuselage length (m)	2.5
Diameter of tail rotor (m)	0.3
Rotor/wing area (m^2)	0.19
Canard area (m^2)	0.30
Horizontal tail area (m^2)	0.32
Take-off weight (kg)	13.28

the position of vertical to the fuselage as a fixed wing surface. Then, the lift generated by the three wings are redistributed to ensure that the CRW can obtain an economic cruise layout in fixed-wing mode.

B. FLIGHT DYNAMICS MODELLING OF TRANSITION MODE FOR THE CRW AIRCRAFT

The main parameters of the CRW studied in this paper (Fig. 1) are listed in table 1.

Based on the transition scheme designed in the previous section, the aerodynamic models of the main rotor and the tail rotor systems were developed by mechanism analysis, and the aerodynamic forces and moments of those fixed wings and fuselage under complex aerodynamic interaction were calculated by CFD. The dynamic derivatives are concerned by engineering estimation.

First, body frame fixed to the airplane is defined. The origin O is at the aircraft's centre of gravity, the x axis is parallel to the geometrical horizontal fuselage datum, y axis is aligned to the starboard and z axis is directed "downwards". According to Newton's law and the momentum moment theorem, the dynamics equations of the aircraft under the body frame [15], [16] can be written as follows:

$$\begin{aligned} F_x &= m\,(\dot{u} + qw - rv) \\ F_y &= m\,(\dot{v} + ru - pw) \\ F_z &= m\,(\dot{w} + pv - qu) \end{aligned} \tag{1}$$

$$\begin{aligned} M_x &= \dot{p}I_x - \dot{r}I_{xz} + qr(I_z - I_y) - pqI_{xz} \\ M_y &= \dot{q}I_y + pq(I_x - I_z) + (p^2 - r^2)I_{xz} \\ M_z &= \dot{r}I_z - \dot{p}I_{xz} + pq(I_y - I_x) + qrI_{xz} \end{aligned} \tag{2}$$

where m is the aircraft mass, u, v, and w are the components of the flight velocity on the x, y and z axes of the body axis system, q, p and r are the pitch rate, roll rate and yaw rate, respectively, I_x, I_y, and I_z are the moments of inertia. I_{xz} is the product of inertia. F_x, F_y, and F_z are the resultant forces on the x, y, and z axes, respectively. M_x, M_y and M_z are the resultant moments of the x, y, and z axes.

The resultant force and moment acting on the centre of gravity of the aircraft are

$$\begin{bmatrix} F_x \\ F_y \\ F_z \end{bmatrix} = \begin{bmatrix} F_x \\ F_y \\ F_z \end{bmatrix}_{mr} + \begin{bmatrix} F_x \\ F_y \\ F_z \end{bmatrix}_{tr} + \begin{bmatrix} F_x \\ F_y \\ F_z \end{bmatrix}_{cw+ht+vt+f} \tag{3}$$

$$\begin{bmatrix} M_x \\ M_y \\ M_z \end{bmatrix} = \begin{bmatrix} M_x \\ M_y \\ M_z \end{bmatrix}_{mr} + \begin{bmatrix} M_x \\ M_y \\ M_z \end{bmatrix}_{tr} + \begin{bmatrix} M_x \\ M_y \\ M_z \end{bmatrix}_{cw+ht+vt+f} + \begin{bmatrix} M_x \\ M_y \\ M_z \end{bmatrix}_{Ail} + \begin{bmatrix} M_x \\ M_y \\ M_z \end{bmatrix}_{Rud} + \begin{bmatrix} M_x \\ M_y \\ M_z \end{bmatrix}_{Ele} \tag{4}$$

where the subscripts denote the following: main rotor (mr), tail rotor (tr), canard wing + horizontal tail + vertical tail + fuselage (cw + ht + vt + f), aileron (Ail), rudder (Rud) and elevator (Ele).

The angular motion equations are

$$\begin{aligned} \dot{\varphi} &= p + \tan\theta(q\sin\varphi + r\cos\varphi) \\ \dot{\theta} &= q\cos\varphi - r\sin\varphi \\ \dot{\psi} &= \frac{q\sin\varphi + r\cos\varphi}{\cos\theta} \end{aligned} \tag{5}$$

where θ, φ, and ψ are the pitch angle, roll angle and yaw angle, respectively. Equations (1), (2), and (5) collectively represent the flight dynamics model of transition mode employed in this study.

(1) Aerodynamic models of the main rotor and tail rotor

The axis system of the rotor hub is defined as follows: The origin is at the centre of the rotor hub; the z axis is directed downwards along the rotation axis of the main rotor; the y axis is aligned to the starboard, vertically to the rotation axis;

and the x axis is set according to the right-hand law. The rotor hub of the CRW aircraft is in the form of a seesaw with constraints, thus, the aerodynamic forces and moments generated by the main rotor relative to the centre of gravity of the CRW are

$$\begin{bmatrix} F_x \\ F_y \\ F_z \end{bmatrix}_{mr} = R_h^b \begin{bmatrix} -H_h \\ S_h \\ -T_{mr} \end{bmatrix} \tag{6}$$

$$\begin{bmatrix} M_x \\ M_y \\ M_z \end{bmatrix}_{mr} = R_h^b \begin{bmatrix} L_h \\ M_h \\ -Q_{mr} \end{bmatrix} + r_h \times \begin{bmatrix} F_x \\ F_y \\ F_z \end{bmatrix}_{mr} \tag{7}$$

where R_h^b is the transform matrix from the hub axis system to the body axis system, and r_h is the representation axis of the radius vector from the centre of aircraft gravity to the main rotor hub in the body axis system, H_h, S_h, and T_{mr} denote the backward force, lateral force and thrust of the main rotor in the hub axis system, respectively, L_h and M_h denote the rolling moment and pitching moment in the hub axis system generated by main rotor flapping, Q_{mr} is the anti-torque generated by the main rotor.

The aerodynamic forces H_h, S_h, T_{mr} and aerodynamic moments L_h, M_h, Q_{mr} of the main rotor can be solved by blade element theory [11], [12], the details of the calculation can be found in [11], [17]– [19].

The tail rotor system has no automatic swashplate and only collective pitch can be adjusted. For the miniature helicopter in this study, the flap motion of the tail rotor can be ignored, and only the rotor thrust T_{tr} and anti-torque Q_{tr} are considered. The solution process can refer to that of the main motor thrust T_{mr} and anti-torque Q_{mr}. The resultant force and moment acting on the aircraft's centre of gravity by the tail rotor are

$$\begin{bmatrix} F_x \\ F_y \\ F_z \end{bmatrix}_{tr} = \begin{bmatrix} 0 \\ T_{tr} \\ 0 \end{bmatrix} \tag{8}$$

$$\begin{bmatrix} M_x \\ M_y \\ M_z \end{bmatrix}_{tr} = \begin{bmatrix} 0 \\ Q_{tr} \\ 0 \end{bmatrix} + r_{h\_tr} \times \begin{bmatrix} F_x \\ F_y \\ F_z \end{bmatrix}_{tr} \tag{9}$$

where r_{h_tr} is the radius vector from the aircraft's centre of gravity to the hub centre of the tail rotor in the body axis system.

(2) Aerodynamic model of the fuselage, canard wing, horizontal tail, elevator, aileron, vertical tail and rudder

To consider both the fixed-wing mode and helicopter mode, the CRW aircraft has a unique aerodynamic layout [20] (Fig. 1 and Fig. 2). Calculations of the aerodynamic force and moment of the fuselage, canard wing, horizontal tail, vertical tail at different AOA and sideslip angles, as well as the aerodynamic moment of the elevator, aileron and rudder at different deflections were performed by CFD. The aerodynamic downwash of the main rotor on these components is also taken into account. The dynamic derivatives are obtained through engineering estimation [21].

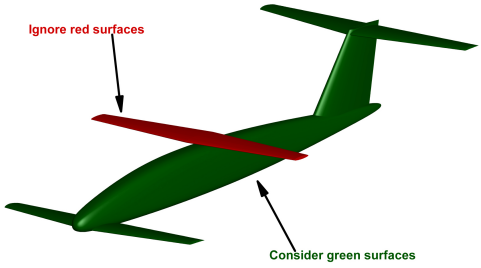

FIGURE 4. Geometry used in CFD calculation.

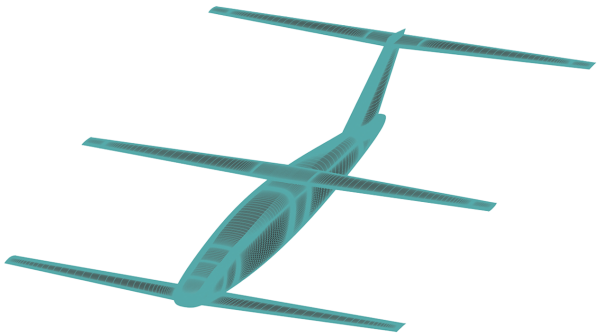

FIGURE 5. The surface grids of the CRW aircraft.

The geometry used in CFD calculation is shown in Fig. 4 while the far field boundary was set 50 times of the main rotor radius away from the centre of gravity. Structured 1 to 1 grids were created to discrete the computational domain. Total grid points number is 34 million. First cell size in wall boundary layer was set small enough to keep y-plus of the surface grid less than 1. The surface grids are shown in Fig. 5.

CFL3D numerical code developed by NASA langley research center was employed to solve the flow around CRW. Reynold Average Navier-Stokes (RANS) equations combined with Spalart-Allmaras turbulence model were solved numerically by finite volume method. The solutions presented herein were obtained using MUSCL reconstruction on the convective fluxes with the Roe upwind scheme. Approximate factorization method was used in the implicit time marching. In addition, CFL3D flow solver has been widely validated with different cases in aeronautical applications [22]– [25].

Boundary conditions are set as adiabatic no slip wall on the wall surfaces and freestream characteristic conditions based on Riemann invariants on the far field surfaces.

After calculating CRW with the configuration in Fig. 4, the results of the resultant aerodynamic forces and moments of the canard wing, horizontal tail, vertical tail and fuselage under the aerodynamic downwash of the main rotor at different AOA and sideslip angles are presented in Fig. 6. The aerodynamic coefficients of the elevator, aileron, rudder at different deflections are shown in Fig.7.

In Fig. 6, C_{Fx}, C_{Fy}, and C_{Fz} are the longitudinal force coefficient, lateral force coefficient and normal force coef-

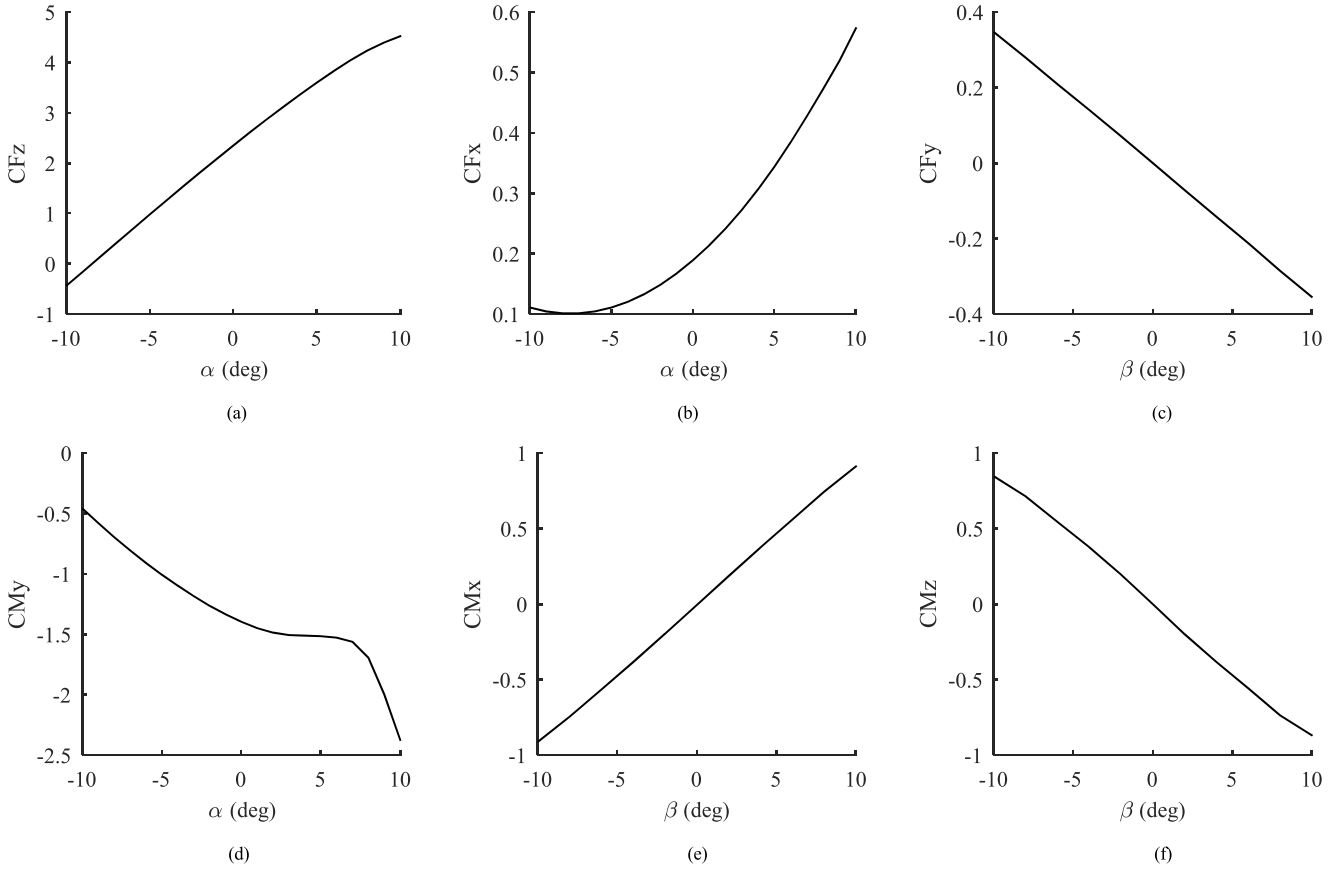

FIGURE 6. The resultant aerodynamic force and moment coefficients of the fuselage, canard wing, horizontal tail and vertical tail at different AOA and sideslip angles during the transition process. (a) Lift coefficient. (b) Drag coefficient. (c) Side force coefficient. (d) Pitching moment coefficient. (e) Rolling moment coefficient. (f) Yaw moment coefficient.

ficient, respectively. C_{Mx}, C_{My}, and C_{Mz} are the roll moment coefficient, pitch moment coefficient and yaw moment coefficient, respectively.

According to the aerodynamic force and moment coefficients in Fig. 6 and Fig. 7, the aerodynamic forces and moments of the fuselage, canard wing, horizontal tail, vertical tail, elevator, aileron and rudder of the CRW under the aerodynamic interaction of the main rotor during transition can be denoted as

$$\begin{bmatrix} F_x \\ F_y \\ F_z \end{bmatrix}_{\text{(cw+ht+vt+f)\_static}} = \frac{1}{2}\rho V^2 S \begin{bmatrix} C_{Fx} \\ C_{Fy} \\ C_{Fz} \end{bmatrix} \tag{10}$$

$$\begin{bmatrix} M_x \\ M_y \\ M_z \end{bmatrix}_{\text{(cw+ht+vt+f)\_static}} = \begin{bmatrix} \frac{1}{2}\rho V^2 SbC_{Mx} \\ \frac{1}{2}\rho V^2 ScC_{My} \\ \frac{1}{2}\rho V^2 SbC_{Mz} \end{bmatrix} \tag{11}$$

$$\begin{bmatrix} M_x \\ M_y \\ M_z \end{bmatrix}_{\text{Ail}} + \begin{bmatrix} M_x \\ M_y \\ M_z \end{bmatrix}_{\text{Rud}} + \begin{bmatrix} M_x \\ M_y \\ M_z \end{bmatrix}_{\text{Ele}} = \frac{1}{2}\rho V^2 Sc \begin{bmatrix} 0 \\ C_{My\_ele} \\ 0 \end{bmatrix} + \frac{1}{2}\rho V^2 Sb \begin{bmatrix} C_{Mx\_Ail} + C_{Mx\_Rud} \\ 0 \\ C_{Mz\_Rud} \end{bmatrix} \tag{12}$$

where ρ is the air density, S is the reference area and takes the area of the main rotor here, c is the average aerodynamic chord length, b is the wingspan, V is flight velocity, the subscript "static" denote the aerodynamic force and moment generated by static derivatives.

It is very complicated to get the dynamic derivatives by CFD or wind tunnel test. Therefore, the paper obtains dynamic derivatives by engineering estimation [21]. The aerodynamic layout used in estimation is as shown in Fig. 8. In the estimation, the main rotor is neglected, and the downwash of the canard wing to the horizontal tail and vertical tail is considered. The estimation results are as shown in table 2.

The reference variables adopted in table 2 are same as C_{Fx}, C_{Fy}, C_{Fz}, C_{Mx}, C_{My}, and C_{Mz}. The aerodynamic forces

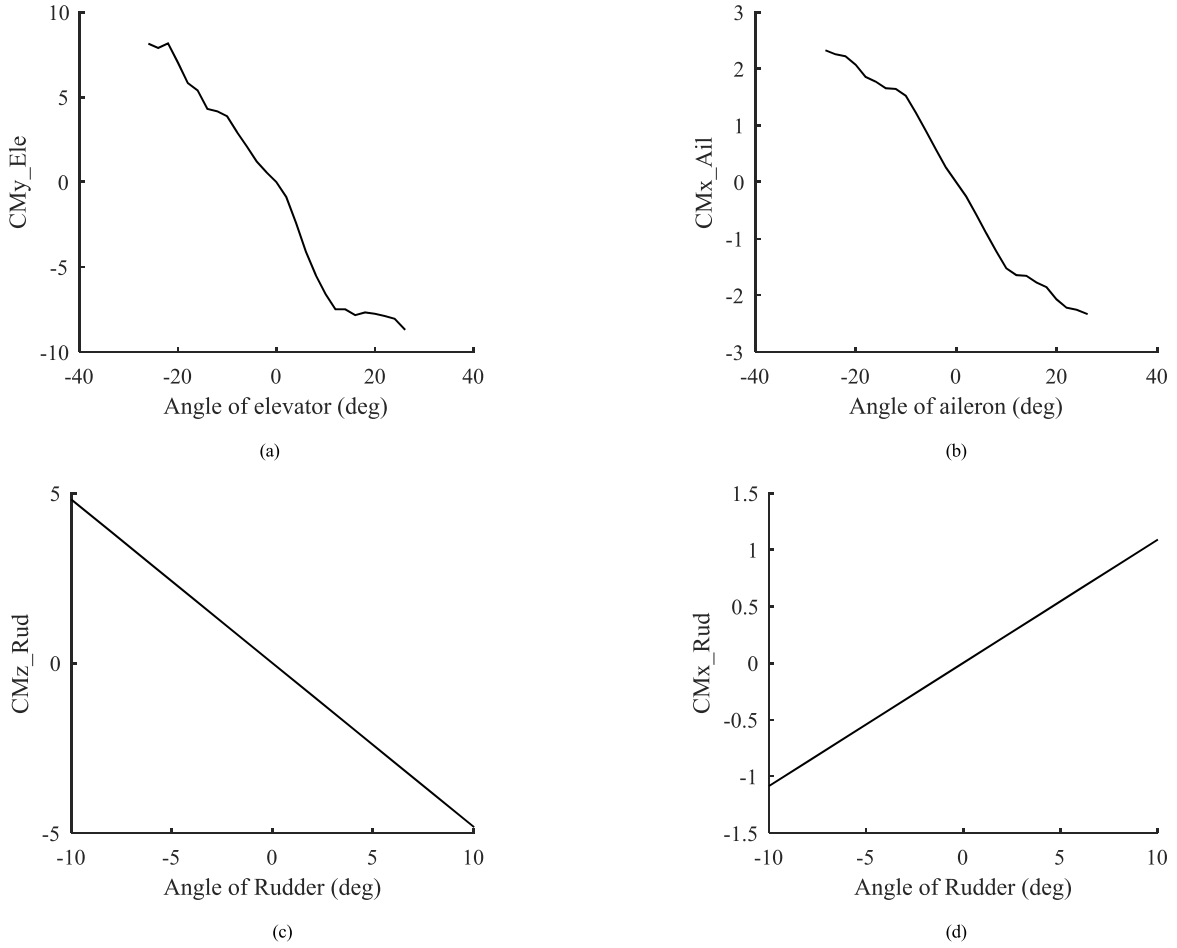

FIGURE 7. Aerodynamic moment coefficients of the elevator, aileron, and rudder at different deflections. (a) Pitching moment coefficient. (b) Rolling moment coefficient. (c) Yaw moment coefficient. (d) Rolling moment coefficient.

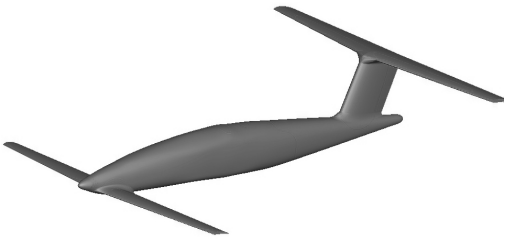

FIGURE 8. The aerodynamic layout used in engineering estimation.

TABLE 2. Estimation results of the dynamic derivatives.

Dynamic derivatives	Value
pitching moment versus pitch rate	-171.04
lift versus pitch rate	-5.46
pitching moment versus AOA rate	-19.03
lift versus AOA rate	-3.29
rolling moment versus roll rate	-0.27
rolling moment versus yaw rate	0.14
yaw moment versus roll rate	-0.02
yaw moment versus yaw rate	-0.56

and moments generated by the dynamic derivatives can be calculated referring to equations 10 and 11.

III. TRIM DURING TRANSITION

The purpose of trim is to determine the appropriate control variables and state variables that can make the resultant force and moment of the aircraft zero. For the transition process, the main sources of aerodynamic lift are the main rotor, canard wing and horizontal tail. The aerodynamic moment can either be adjusted by the control system of helicopter or the fixed-wing control surfaces. Because of being dynamic transfer of lift components and redundancy of control system during transition, it is necessary to design a reasonable trimming scheme to make the transition process smooth and steady.

A. TRIM OF LIFT DURING TRANSITION

The transition scheme designed in the last chapter is that the CRW maintains straight flight at a constant altitude with its AOA being zero, therefore, the local AOA of the canard wing and horizontal tail are the installation angles. Thus, there exists a one-to-one correspondence between the lift produced by the canard wing and horizontal tail and the

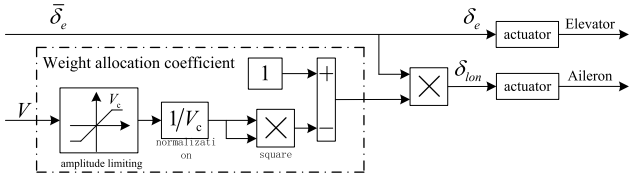

FIGURE 9. Weight allocation of the longitudinal cyclic pitch and elevator during transition.

forward flight speed. For a concrete transition flight speed, the lift produced by the fixed wings is definite, and the main rotor only needs to provide the rest lift to maintain straight flight at a constant altitude. Thrust of the main rotor can be adjusted by regulating the collective pitch, therefore, based on the transition scheme proposed, the trim strategy of lift during the transition is to regulate the collective pitch to make the total lift of the canard wing, horizontal tail and the main rotor equal to the weight of the aircraft.

B. TRIM OF MOMENT DURING TRANSITION

The trim strategy of moment is designed by analyzing the sources of unbalanced moments and follows the principle of ''who produces, who trims''. The principle denotes that if the unbalanced moment generated by the helicopter system in transition, then, the trimming of moment is only by the control system of helicopter, and the fixed-wing control surfaces don't participate in trimming, vice versa. If both the helicopter system and fixed-wing system contribute to the unbalanced moment, the two sets of control systems are involved in trimming.

(1) During the transition process from helicopter in hover to fixed-wing flight mode, with increasing flight speed, the main rotor falling toward backwards and generates pitch moment, meanwhile the increasing lift of the fixed wing also generates pitch moment due to non-coincidence between the aerodynamic center and center of gravity. As both the helicopter system and fixed-wing system generate pitch moments, according to the theory of ''who produces, who trims'' proposed in this chapter, longitudinal cyclic pitch and elevator are used in trimming the pitch moment. Thus redundancy appears in the longitudinal trim. Weight allocation is required to coordinate longitudinal cyclic pitch and elevator to achieve trimming. The forward flight speed increases with the transition process, and The efficiency of the elevator gradually increases with the increasing speed, i.e., the trim capability of the elevator. The trim capability of the longitudinal cyclic pitch need to be weakened so as to keep the trim ability invariant. Weight allocation of the longitudinal cyclic pitch and elevator is implemented with the variation of forward flight speed during the transition process, as shown in Fig. 9.

In Fig. 9, $\bar{\delta}_e$ is the nominal pitch input, δ_e is the elevator control input, δ_{lon} is the longitudinal cyclic pitch input, V_c is the speed of the CRW at the end of the transition process, the dotted-line frame represents the weight coefficient of longitudinal cyclic pitch. Variation of the weight for δ_{lon} with

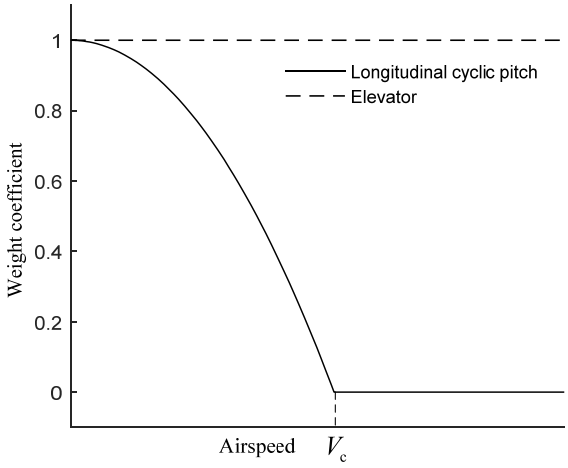

FIGURE 10. Weight coefficient of longitudinal cyclic pitch and elevator with forward flight speed during the transition process.

the transition speed V is shown in Fig. 10 after processing according to Fig. 9.

(2) The fixed-wing system is symmetrically distributed along the symmetry plane of the aircraft and it does not generate roll and yaw moments during the transition process, so the aileron and rudder do not participate in trimming the roll and yaw moment, and only the lateral cyclic pitch, roll angle and tail collective pitch are involved.

IV. THE CONTROL MODEL DURING TRANSITION

The initial state of CRW transition is hovering in helicopter mode, and the control command acts on the helicopter control system. At the end of the transition, it is fixed-wing flight mode and the control command acts on the fixed-wing control system. During the transition flight of the CRW, the helicopter control system and the fixed-wing control surfaces are all involved in the operation, which results in the control redundancy. In order to eliminate the control redundancy in the transition process and realize the smooth transfer of the command from the helicopter control system to the fixed-wing control system, it is necessary to establish a supplementary control model for the two sets of control systems during the transition.

To design the control model, finding a variable that can represent the maneuver ability of each control system in different states of the transition process should be done first [26]. In this section, the dimensional control derivative is used to characterize the operation capability of each control input. Then, the control model is designed based on the total manipulation ability of the two sets of control systems during the transition process according to a certain law.

The study in this section is based on the transition scheme proposed in Section II-A. Assuming that the acceleration in the transition flight is very small, close to zero, and the CRW can be considered in steady-state flight during the transition. In this way, a small perturbation linearization method can be used to study the control model. Based on this assumption, several state points of the transition process are selected, and

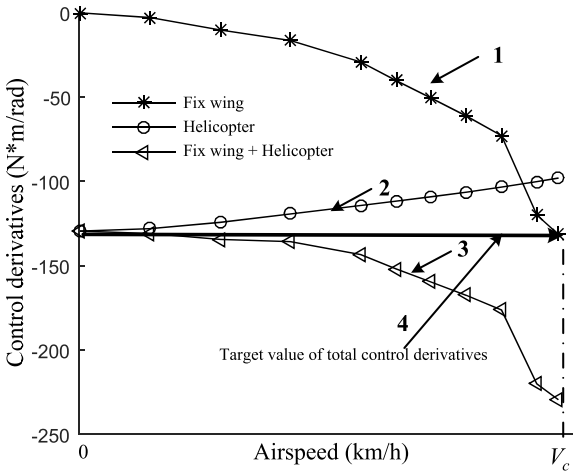

FIGURE 11. Variation trend of control derivatives of helicopter and fixed-wing in transition process.

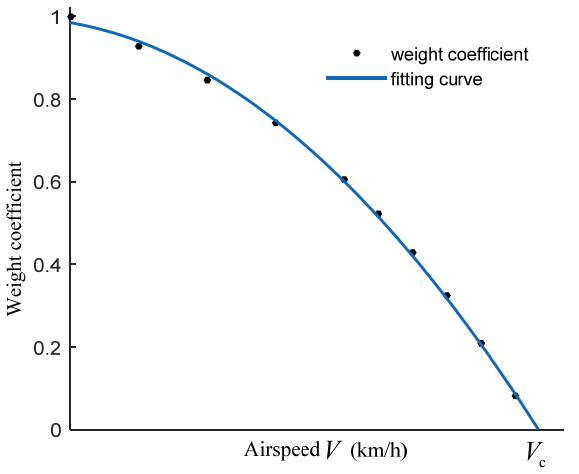

FIGURE 12. Weight coefficient of the control input of helicopter during transition.

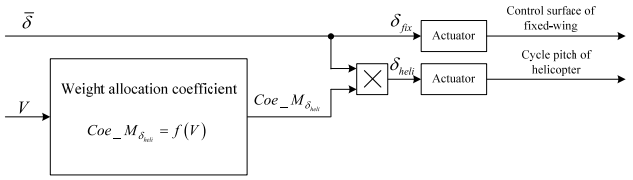

FIGURE 13. Single-channel control Model.

the flight dynamics model of the CRW transition mode established in this paper is used to linearization. Then, the dimensional control derivatives can be obtained.

Suppose there are two control inputs for a control channel of CRW during transition: helicopter control input δ_{heli} and fixed-wing control input δ_{fix}, and the beginning of transition is helicopter mode operated by δ_{heli}. At the end of the transition, the fixed-wing mode is manipulated by the δ_{fix}, and both δ_{heli} and δ_{fix} are involved in the transition. The control derivatives $M_{\delta_{heli}}$ and $M_{\delta_{fix}}$ corresponding to the control input δ_{heli} and δ_{fix} in the transition process are shown in curve 2 and curve 1 in Fig. 11, respectively. Curve 3 is the sum of curve 1 and curve 2, indicating the overall manipulation ability in the transition process. The issue of establishing a transition control model can be described as: by designing a control model, realizing smooth transition from the control derivative $M_{\delta_{heli}0}$ of helicopter mode at the start of the transition (value of curve 2 at 0 airspeed speed in Fig. 11) to fixed-wing mode with control derivative $M_{\delta_{fix}0}$ (value of curve 1 at V_c airspeed in Fig. 11). In this paper, we first design the changing rule of the control ability during transition, as shown in the curve 4 in Fig. 11, that is, the control ability changes linearly from the beginning of the transition to the end of the transition, and then design the control model based on the target control ability. Thus, the smooth transfer of the control authority in the transition process is realized.

The dimensional control derivative (curve 1) of the fixed-wing changes automatically with the increase of forward flying velocity during the transition. For the sake of simplicity, in this study, only the value of helicopter control derivative (curve 2) is adjusted so that the total control derivative (curve 3) changes according to the rule of curve 4 in Fig. 11. The design detail is as follows: using curve 3 in Fig. 11 minus curve 1, and the target value of helicopter control derivative during the transition process is obtained. Then divided by the actual helicopter control derivative (curve 2) for dimensionless transformation, the weight coefficient of helicopter control input is obtained, as shown in Fig. 12.

The corresponding fitting formula is $Coe\_M_{\delta_{heli}} = f(V)$, where $Coe\_M_{\delta_{heli}}$ is the weight coefficient of helicopter control input, V is the forward flying velocity, and $f(V)$ is the function of velocity V.

Then the control model of the channel can be established, as shown in Fig. 13.

In Fig. 13, $\bar{\delta}$ is the nominal input for the channel. Once the control model is constructed, the two control inputs: δ_{fix} and δ_{heli} will be reduced into a single input $\bar{\delta}$, and the redundancy problem is solved. With the control model, in the transition process, the control ability of the channel becomes curve 4 in Fig. 11, and the smooth transfer of the control authority is realized, which meets the design target.

V. TRIM, CONTROL MODEL, AND STABILITY ANALYSIS OF THE CRW DURING TRANSITION

A. TRIM

For the transition scheme of CRW proposed in this study, trim is performed at different forward flight speeds V from hover to the end of transition. During transition, the CRW maintains straight flight at a constant altitude with zero AOA, the aileron and rudder of fixed-wing do not take part in trimming. The trim results of the state variables and control inputs as well as the main aerodynamic forces and moments generated by the components of helicopter and fixed-wing are shown in Fig. 14.

It is shown in Fig. 14: (1) The roll angle in Fig. 14. (a), mainly to produce the lateral component of the main rotor

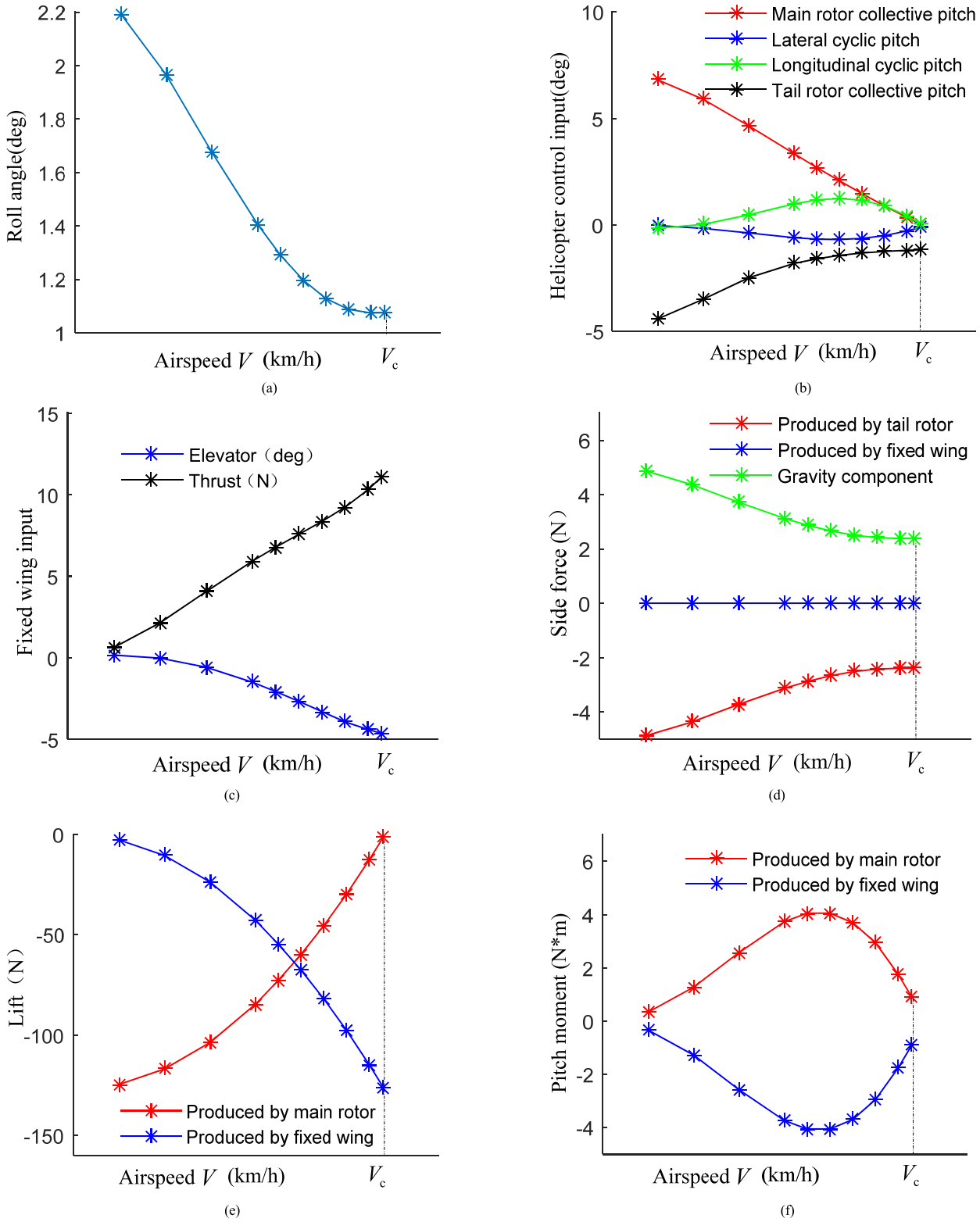

FIGURE 14. Trim results of the CRW at different speeds during transition process. (a) Trim result of roll angle. (b) Trim results of helicopter control input. (c) Trim results of fixed-wing control input. (d) Trim results of side force. (e) Trim results of lift. (f) Trim results of pitch moment.

thrust to trim the lateral force of the tail rotor, it decreases with the increase of transition flight speed. As the lift produced by the canard wing and horizontal tail increases, the thrust required from the main rotor decreases. Thereby, the

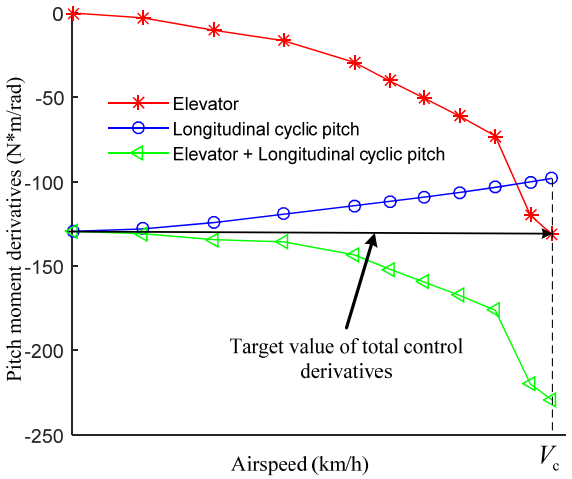

FIGURE 15. Derivatives of the pitch moment to longitudinal cyclic pitch and elevator.

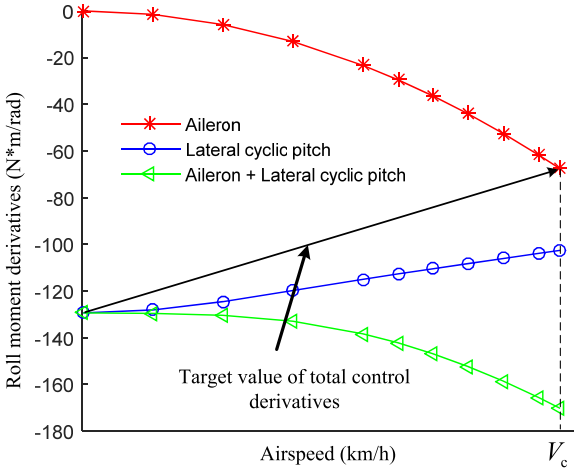

FIGURE 16. Derivatives of the roll moment to lateral cyclic pitch and aileron.

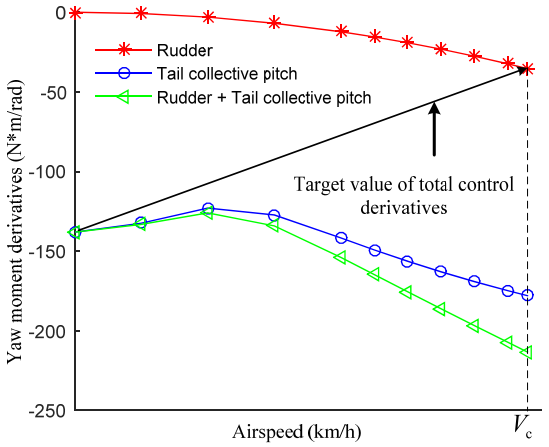

FIGURE 17. Derivatives of yaw moment to tail rotor collective pitch and rudder.

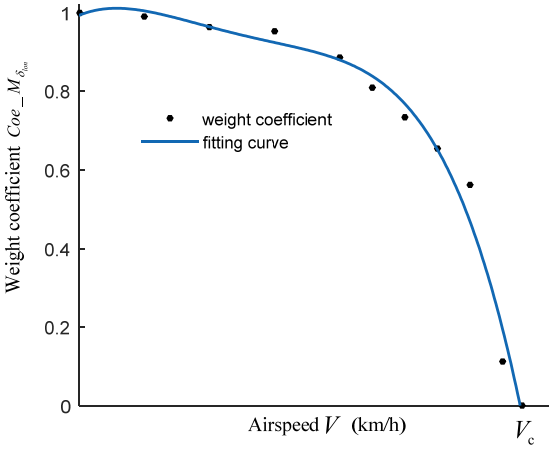

FIGURE 18. Weight coefficient of the pitch moment to the longitudinal cyclic pitch control derivative during transition.

anti-torque of the main rotor reduces, result in the thrust required from the tail rotor decreases. Correspondingly, the trim value of the roll angle decreases too, which is logical and agrees with the trim results in Fig. 14.(d). (2) The Fig. 14.(b) presents that the collective pitch of the main rotor and tail rotor gradually decrease with increasing forward flight speed during the transition process. The main rotor collective pitch decreases to zero at the end of transition and provides no more thrust,
which agrees with the transition scheme designed in the previous chapter. The tail rotor collective pitch still has value when collective pitch of the main rotor equals to zero, as the main rotor still generate anti-torque because of the drag force of rotor still being exist. (3) Fig. 14. (c) demonstrates that deflection of elevator increases with increasing transition speed. As with increasing of dynamic pressure, the nose-down pitching moment produced by the fixed-wing increases, so does the elevator deflection. It can be seen in Fig. 14.(f) that a part of pitch moment is provided by the rotor system in trimming the nose-down pitching moment from the fixed-wing surfaces. (4) Fig. 14. (e) shows that the overall lift source of the CRW in transition shifts smoothly from the rotor system to the fixed-wing surfaces.

B. CONTROL MODEL

The controllable input of the CRW during transition is: $U = [\delta_a\ \delta_e\ \delta_T\ \delta_r\ \delta_{lat}\ \delta_{lon}\ \delta_{ped}\ \delta_{col}]^T$: where δ_a, δ_e and δ_r are control surfaces of aileron, elevator, and rudder from fixed-wing, respectively; δ_{lat}, δ_{lon} and δ_{ped} are the control input of lateral cyclic pitch, longitudinal cyclic pitch and tail collective pitch from helicopter, respectively. Among them, δ_a and δ_{lat} can produce rolling moment, δ_e and δ_{lon} can produce pitch moment, δ_r and δ_{ped} can produce yaw moment. The helicopter mode is controlled by δ_{lat}, δ_{lon}, and δ_{ped} at the start of the transition, and the fixed-wing mode is operated by δ_a, δ_e, δ_r at the end of the transition.

According to the method proposed in this paper, the control model for pitch channel, roll channel and yaw channel of CRW transition is designed. The control derivatives of each control input during transition and the variation

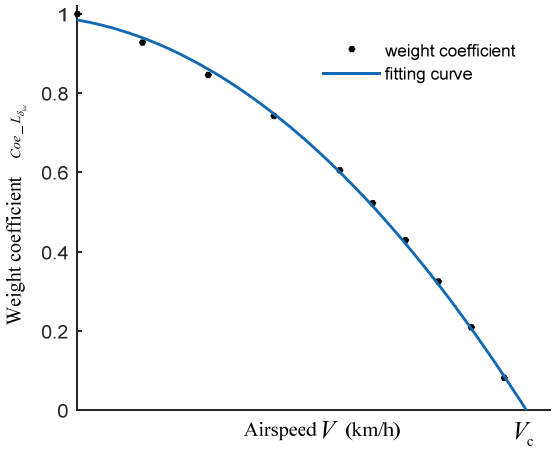

FIGURE 19. Weight coefficient of the roll moment to the lateral cyclic pitch control derivative during transition.

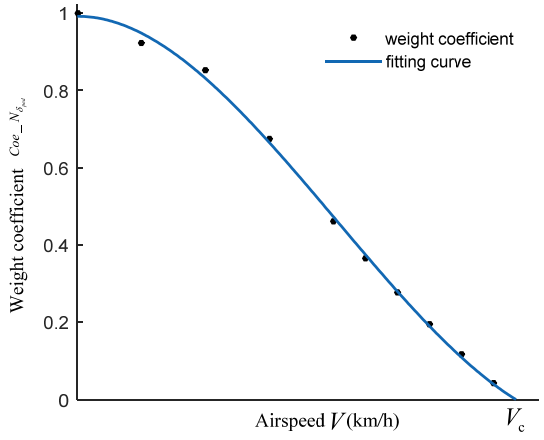

FIGURE 20. Weight coefficient of the yaw moment to the tail rotor collective pitch control derivative during transition.

of the designed target manipulation derivatives are shown in Fig. 15 to Fig. 17.

The weight coefficients of the helicopter control input can be obtained as shown in Fig. 18 to Fig. 20:

The fitting formulas corresponds to Fig. 18 to Fig. 20 are as follows:

$$\begin{aligned} Coe\_M_{\delta_{lon}} &= g(V) \\ Coe\_L_{\delta_{lat}} &= h(V) \\ Coe\_N_{\delta_{ped}} &= t(V) \end{aligned}$$

Therefore, the control model for the pitch channel, roll channel, yaw channel can be established as shown in Fig. 21.

In Fig. 21, $\bar{\delta}_e$, $\bar{\delta}_a$, and $\bar{\delta}_r$ are the nominal control inputs of pitch, roll and yaw, respectively. By establishing the above control model, six control inputs δ_{lon}, δ_{lat}, δ_{ped}, δ_e, δ_a, δ_r are reduced to three: $\bar{\delta}_e$, $\bar{\delta}_a$, $\bar{\delta}_r$, thereby, the longitudinal control input $\bar{\delta}_e$, lateral control input $\bar{\delta}_a$, and yaw control input $\bar{\delta}_r$ correspond to the longitudinal channel, lateral channel and yaw channel, respectively. The control during the transition process becomes simple and efficient.

C. STABILITY ANALYSIS

For the trim points in transition mode, a linearized small perturbation was implemented. Eigenvalues were solved, and variation of the eigenvalues during the transition process is shown in Fig. 22.

It is shown in Fig. 22 that most eigenvalues move towards left along the real axis with increasing flight speed during transition, which indicates that stability of these modes increases. However, two eigenvalues are separated into two real roots from a pair of conjugate complex roots, with the forward flight speed increases, one moves towards the direction of the negative real axis and the stability increases, the other moves along the positive real axis and becomes monotonous divergence mode. However, with further increase of the transition speed, the two eigenvalues moving towards the negative and positive axis both shift direction and intersect again at the end of transition and appear as conjugate complex roots. Their positions are more distant to the imaginary axis compared to the primary conjugate complex roots thus are more stable. The results of complex changes of eigenvalues show

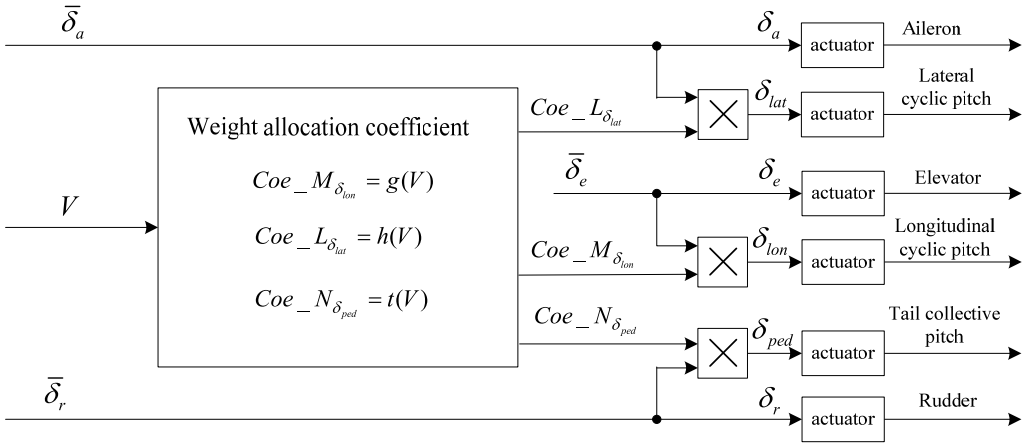

FIGURE 21. Control model for pitch channel, roll channel and yaw channel of the CRW during transition.

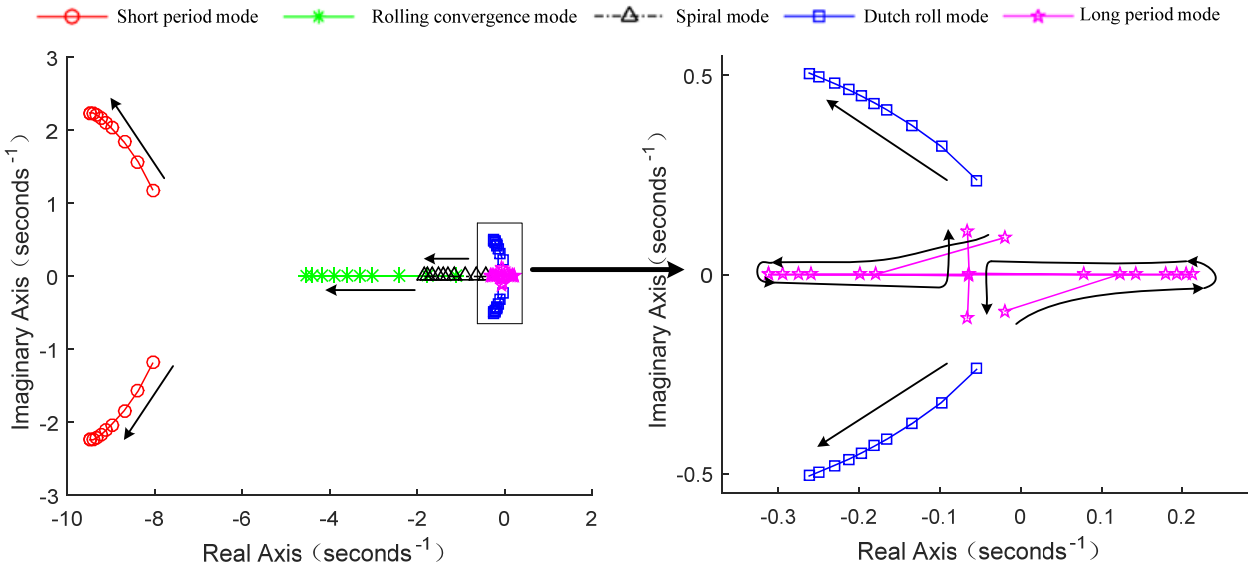

FIGURE 22. Variation of the eigenvalues during transition.

that the stability of CRW in transition mode is complicated, and they are very useful for the overall optimization design and control system design.

VI. CONCLUSIONS

1) A set of transition scheme has been proposed based on flight test experience and features of the CRW aircraft. The scheme is proved to be reasonable and effective from the trim results.

2) A trim strategy has been proposed based on the transition flight principle and has been proved practical by the smooth change of trim variables throughout the transition process. The trim results can guide the overall optimization design of the CRW aircraft.

3) The trim results are credible and reasonable, demonstrating the applicability of the modelling methodology as well as the reliability of the model developed. The model can be employed for the flight dynamics analysis and control system design of the CRW aircraft.

4) The control model proposed can eliminate redundant and enable simple and effective control of the CRW in transition flight, which lays a foundation for the following flight control system design.

5) Linearized small perturbation has been implemented at trim points for the transition model, and the variation trends of eigenvalues with transition speed have been analyzed. Deeper comprehension of the CRW characteristics during transition is acquired which can provide guidance for the overall design and control system design.

In all, the work described in the paper provides a set of solution to the model building, trim, control model design and the stability analysis of CRW aircraft in transition mode. The results will lay a foundation for the following overall optimization design and control system design. My further work is to design a flight control system to achieve autonomous flight of the CRW.

REFERENCES

[1] C. Mitchell and B. Vogel, "The canard rotor wing (CRW) aircraft—A new way to fly," in *Proc. AIAA/ICAS Int. Air Space Symp. Expo., Next 100 Years*, Dayton, OH, USA, 2003, pp. 1–11.

[2] Y.-P. Deng, Z.-H. Gao, and H. Zhan, "Development and key technologies of the CRW," *Flight Dyn.-Xian*, vol. 24, no. 3, p. 1, Sep. 2006.

[3] C. A. Lopez and V. L. Wells, "Dynamics and stability of an autorotating rotor/wing unmanned Aircraft," *J. Guid., Control, Dyn.*, vol. 27, no. 2, pp. 258–270, 2004.

[4] S. Bass, T. Thompson, J. Rutherford, and S. Swanson, "Low-speed wind tunnel test results of the Canard Rotor/Wing concept," in *Proc. 11th Appl. Aerodyn. Conf.*, Monterey, CA, USA, 1993, p. 3412.

[5] A. He, Z. H. Gao, and Y. P. Deng, "Dynamic experimental study on the effect of rotary wing on the aerodynamic characteristics of CRW," *J. Exp. Fluid Mech.*, vol. 27, no. 3, pp. 13–16, Jun. 2013.

[6] Y. P. Deng, Z. H. Gao, and H. Zhan, "Research on aerodynamic interference of hover and fly in small speed of canard rotor/wing aircraft," *J. Experim. Mech.*, vol. 24, no. 6, pp. 563–567, Dec. 2009.

[7] W. Sun, Z. Gao, Y. Du, and F. Xu, "Mechanism of unconventional aerodynamic characteristics of an elliptic airfoil," *Chin. J. Aeronaut.*, vol. 28, no. 3, pp. 687–694, Mar. 2015.

[8] W. Sun, Z. H. Gao, and J. T. Huang, "Research on aerodynamic characteristics of rotary wing," *Acta Aerodynamica Sinica*, vol. 33, no. 2, pp. 232–238, Apr. 2015.

[9] S. Pandya and M. Aftosmis, "Computation of external aerodynamics for a canard rotor/wing aircraft," in *Proc. 39th AIAA Aerosp. Sci. Meeting Exhibit*, Reno, NV, USA, 2001, pp. 1–9.

[10] C. Kong, J. Park, and M. Kang, "A study on transient performance characteristics of the canard rotor wing type unmanned aerial vehicle propulsion system during flight mode transition," *J. Eng. Gas Turbines Power*, vol. 128, no. 3, pp. 573–578, Jul. 2006.

[11] P. D. Talbot, B. E. Tinling, W. A. Decker, and R. T. Chen, "A mathematical model of a single rotor helicopter for piloted simulation," NASA, Washington, DC, USA, NASA Tech. Memorandum 84281, 1982.

[12] S. C. Wang, *Helicopter Aerodynamics*. Nanjing, China: Nanjing Institute of Aeronautics Printing Factory, 1985, pp. 1–180.

[13] W.-D. Gai, H.-L. Wang, and D.-W. Li, "Flight dynamic modeling and analysis for the Canard Rotor/Wing UAV," *Acta Aerodynamica Sinica*, vol. 30, no. 2, pp. 244–249, Apr. 2012.

[14] H. Zhan, Y.-P. Deng, and Z.-H. Gao, "Investigation on aerodynamics performance of elliptic airfoil at low speed," *Aeronautical Comput. Technique*, vol. 38, no. 3, pp. 25–27, May 2008.

[15] Z. P. Fang and W. C. Chen, *Aircraft Flight Dynamics*. Beijing, China: Beihang Univ. Press, 2015, pp. 174–203.
[16] B. Wang, X. Yu, L. Mu, and Y. Zhang, "Disturbance observer-based adaptive fault-tolerant control for a quadrotor helicopter subject to parametric uncertainties and external disturbances," *Mech. Syst. Signal Process.*, vol. 120, pp. 727–743, Apr. 2019.
[17] R. W. Prouty, *Helicopter Performance, Stability, and Control*. Melbourne, FL, USA: Krieger, 1995.
[18] R. T. Chen, "Effects of primary rotor parameters on flapping dynamics," NASA, Washington, DC, USA, NASA Tech. Rep. 1431, 1980.
[19] Z. Gao and R. L. Chen, *Helicopter Flight Dynamics*. Nanjing, China: Science Press, 2003, pp. 43–65.
[20] Z. X. Shi and Z. H. Gao, "Analysis of unloading characteristics of the canard rotary wing airplane blade in transitional process," *Flight Dyn.*, vol. 32, no. 4, pp. 298–302, Aug. 2014.
[21] *Aircraft Design Handbook: Aerodynamic Design*. Aeronautical Ind. Press, Beijing, China, 2002, vol. 6, pp. 382–431.
[22] M. A. Park, K. R. Laflin, M. S. Chaffin, N. Powell, and D. W. Levy, "CFL3D, FUN3D, and NSU3D contributions to the fifth drag prediction workshop," *J. Aircr.*, vol. 51, no. 4, pp. 1268–1283, 2014.
[23] M. Mori *et al.*, "Reynolds-averaged Navier–Stokes technology for transonic drag prediction: A boeing perspective," *J. Aircr.*, vol. 51, no. 4, pp. 1118–1134, 2014.
[24] J. Rodio, X. Xiao, H. A. Hassan, and C. L. Rumsey, "NASA trapezoidal wing simulation using stress-w and one-and two-equation turbulence model," in *Proc. 52nd AIAA Aerosp. Sci. Meeting*, Reston, VA, USA, 2014, pp. 1–19.
[25] E. N. Tinoco, O. Brodersen, S. Keye, and K. Laflin, "Summary of data from the sixth AIAA CFD drag prediction workshop: CRM cases 2 to 5," in *Proc. 55th AIAA Aerosp. Sciences Meeting*, Grapevine, TX, USA, 2017, pp. 1–43.
[26] B. Wang and Y. Zhang, "An adaptive fault-tolerant sliding mode control allocation scheme for multirotor helicopter subject to simultaneous actuator faults," *IEEE Trans. Ind. Electron.*, vol. 65, no. 5, pp. 4227–4236, May 2018.

HONGGANG GAO was born in Shaanxi, China, in 1987. He received the B.S. degree in automation from the Xi'an University of Technology, Xi'an, China, in 2010, and the M.S. degree in control theory and control engineering from Northwestern Polytechnical University, Xi'an, in 2013, where he is currently pursuing the Ph.D. degree in flight dynamics and control with the School of Aeronautics. His research interests include modeling, flight identification, flight dynamics, flight control, and simulation.

ZHENGHONG GAO was born in Gansu, China, in 1960. She received the B.S., M.S., and Ph.D. degrees in aerodynamics from Northwestern Polytechnical University, Xi'an, China, in 1981, 1984, and 1989, respectively.

From 1992 to 1994, she was a Postdoctoral Researcher with the Institute of Aerodynamics and Fluid Mechanics, Technical University of Munich, Germany. She is currently a Professor with the School of Aeronautics, Northwestern Polytechnical University, Xi'an. Her current research interests include the multidisciplinary design optimization of aircraft, flight dynamics, and aerodynamics.

Dr. Gao is a Committee Member of the International Council of the Aeronautical Sciences, and the Executive Director of China Society of Aeronautics and Astronautics and of the China Aerodynamic Association.

YANG NA was born in Liaoning, China, in 1994. He received the B.S. degree in aircraft design and engineering from Northwestern Polytechnical University, Xi'an, China, in 2017. He is currently pursuing the M.S. degree in aircraft design from Northwestern Polytechnical University, Xi'an, China. He is also pursuing the master's student in flight dynamics and control with the School of Aeronautics, Northwestern Polytechnical University. His research interests include modeling, flight identification, flight dynamics, flight control, simulation and aircraft, and engine matching.

CHAO PANG was born in Shaanxi, China, in 1994. He received the B.S. degree in aircraft design and engineering from Northwestern Polytechnical University, Xi'an, China, in 2016, where he is currently pursuing the Ph.D. degree in flight vehicle design with the School of Aeronautics. His research interests include rotorcraft design, computational fluid dynamics, and unsteady aerodynamics.